# Flame Chemistry of Halon Replacements: Low Pressure Studies of C_3F_8 and CF_3I Doped CH, Flames

Andrew McIlroy and Lee K. Johnson
Mechanics and Materials Technology Center
The Aerospace Corporation
P. O. Box 92957/M5-754
Los Angeles, California 90009-2957

Introduction

Since their discovery in the 1950's, the halons have provided excellent protection against fire in a wide variety of applications ranging from computer rooms to military aircraft. The halons embody a critical set of properties including low fire extinguishing concentration, low toxicity and chemical and electrical inertness. Due in part to their tremendous success, surprisingly little effort has been expended to understand the details of their fire suppression activity or to identify other fire suppressants. Since the signing of the Montreal Protocols, the ban on halon production, and the phase out of their use, there has been renewed interest in finding new fire suppressants. Indeed the urgency of the problem has led to several intensive efforts to identify new candidates and validate their use in various test scenarios. However, the basic mechanisms by which halons and their replacements suppress combustion remains poorly characterized and in some circles controversial.

The halons were identified largely through empirical searches in the mid-1950's. They were unique in their ability to extinguish fires at very low concentrations, typically <5% by volume. Initial investigations showed that the presence of bromine is critical to this high efficiency and that the halogen atoms formed a series with increasing fire suppression activity from fluorine through bromine. Iodine showed performance similar to bromine. The radioactive nature of astatine made it inappropriate for study. Early studies hypothesized that the halogens inhibited the radical chemistry of flames, but had no direct evidence of this property. In the 1970's, Biordi and coworkers completed a landmark study of halon 1301 (CF_3Br) flame chemistry using a low pressure flame and a molecular beam sampling mass spectrometer.[1,2,3,4] Their data indicated a chemical mechanism for halon 1301 flame suppression and again implicated bromine as a key factor. At about the same time, Dixon-Lewis and coworkers undertook experimental and modeling studies to determine the role of bromine atoms in fire suppression and identified several key reactions.[5,6,7] Westbrook undertook a detailed chemical kinetic modeling study of halogen fire suppression following these studies. He developed chemical kinetic mechanisms for HX, CH_3X and CF_3Br (X= Cl, Br, I) fire suppression[8,9,10] Westbrook's model of halon 1301 fire suppression shows good agreement with Biordi and coworkers experimental results. He proposed a key catalytic reaction cycle for halogen fire suppression in which hydrogen atoms are converted to hydrogen molecules

$$H + HBr \rightarrow H_2 + Br$$
$$H + Br_2 \rightarrow HBr + Br$$
$$Br + Br + M \rightarrow Br_2 + M$$
$$\overline{H + H \rightarrow H_2}$$
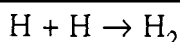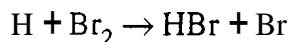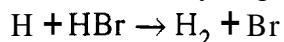
He also identified other possible suppression cycles involving CF, and other radicals. Sheinson and coworkers have presented an elegant analysis which quantifies the relative physical and chemical fire suppression effects of various chemical functional groups." They confirm the earlier fire suppression efficiency ordering of halogen atoms and show that the halons extraordinary fire suppression efficiency must arise from chemical effects. Recently, Battin-Leclerc *et al.* studied the inhibition of methane oxidation by CF_3Br at 1070 K and found the inhibiting influence to be mainly due to Br, HBr and CH_3Br.[12]

Halon replacements can be grossly characterized into three categories: 1) traditional fire fighting agents such as water mists, **2)** inert atmospheres, and **3)** new agents designed to be near drop-in replacements to halons. **This** study concentrates on these latter agents. This group can be broken into two major sub-categories: 1) perfluorocarbons (PFCs) and hydrofluorocarbons (HFCs) which have predominantly physical fire suppression characteristics and **2)** compounds such as CF_3I which show strong chemical fire suppression characteristics typical of the halons.

With recent environmental constraints, the fire protection community has been forced to seek alternatives to halons. Few detailed investigations have been carried out to determine the fire suppression mechanisms of these new agents. At NIST, Westmoreland, Tsang, Burgess and coworkers have developed a detailed reaction mechanism for PFC and HFC combustion, but it has not been rigorously tested against experimental data.[13] Miziolek and coworkers have begun diode laser, low pressure flame studies of HFC chemistry and have found good agreement with the NIST model for the limited number of species investigated to date.[14] Linteris and coworkers have investigated the fire suppression properties of PFCs and HFCs including combustion products and flame speeds and have also found good agreement with flame speeds calculated from the NIST model.[15,16]

We have begun a program of low pressure flame studies employing laser and mass spectrometer diagnostics to compliment and enhance the existing database of fire suppression data on the halon replacement agents. The low pressure flame technique has been chosen for two primary reasons. First the a low pressure, laminar flame is both straight forward to produce in a laboratory and to model. In particular, Kee and coworkers have developed a robust and well validated code for calculating temperature and chemical species profiles for laminar flames." This code includes detailed treatments of one-dimensional transport and chemical kinetics and is based on their CHEMKIN chemical kinetics subroutine package.[18,19,20] Second, a low pressure flame provides access to the full range of combustion temperatures in a single experiment. Other chemical kinetics experimental techniques involving fixed temperature reactors produce excellent data, but are generally limited to temperatures below 1000 K by construction material constraints. The steep temperature dependence of chemical reaction rates makes it imperative to investigate combustion processes in realistic temperatures ranges in order to produce a complete picture of the relevant chemistry.

Experiment

Our low pressure flame apparatus is newly constructed and specifically designed for studies with halogen doped flame. Fig. 1 **shows** an overview of the apparatus. Essentially, all surfaces that come in contact with the flame **gases are** either stainless steel or quartz. Copper gaskets **are** used to seal the ports which experience heat loads and all others **are** sealed with viton **O-rings** The main chamber consists of an six-way, 8" conflat cross. Attached to the bottom of the main chamber is a large three-axis translator. **A** welded steel bellows forms the vacuum wall between the bottom of the chamber and the bottom of the translator. All moving components **are** outside the vacuum chamber to minimize corrosion. The translator has a total vertical travel of ± 25 cm and horizontal travel of ± 5 cm. Horizontal travel is not needed for the experiments described here, but is included in the system for the study of diffusion flames and other reacting flows with two and three dimensional structure. Computer controlled stepper motors provide motion control for the translation stage. The burner is mounted on a stainless steel column attached to the bottom flange of the translator. *All* flame structure experiments **are** carried out with space fied diagnostics and a translating burner assembly. We use a standard McKenna porous plug, flat-flame burner with a sintered stainless steel center frit *6.0* cm in diameter designed for low pressure use. **Gases** and cooling water **are** fed in through the bottom flange.
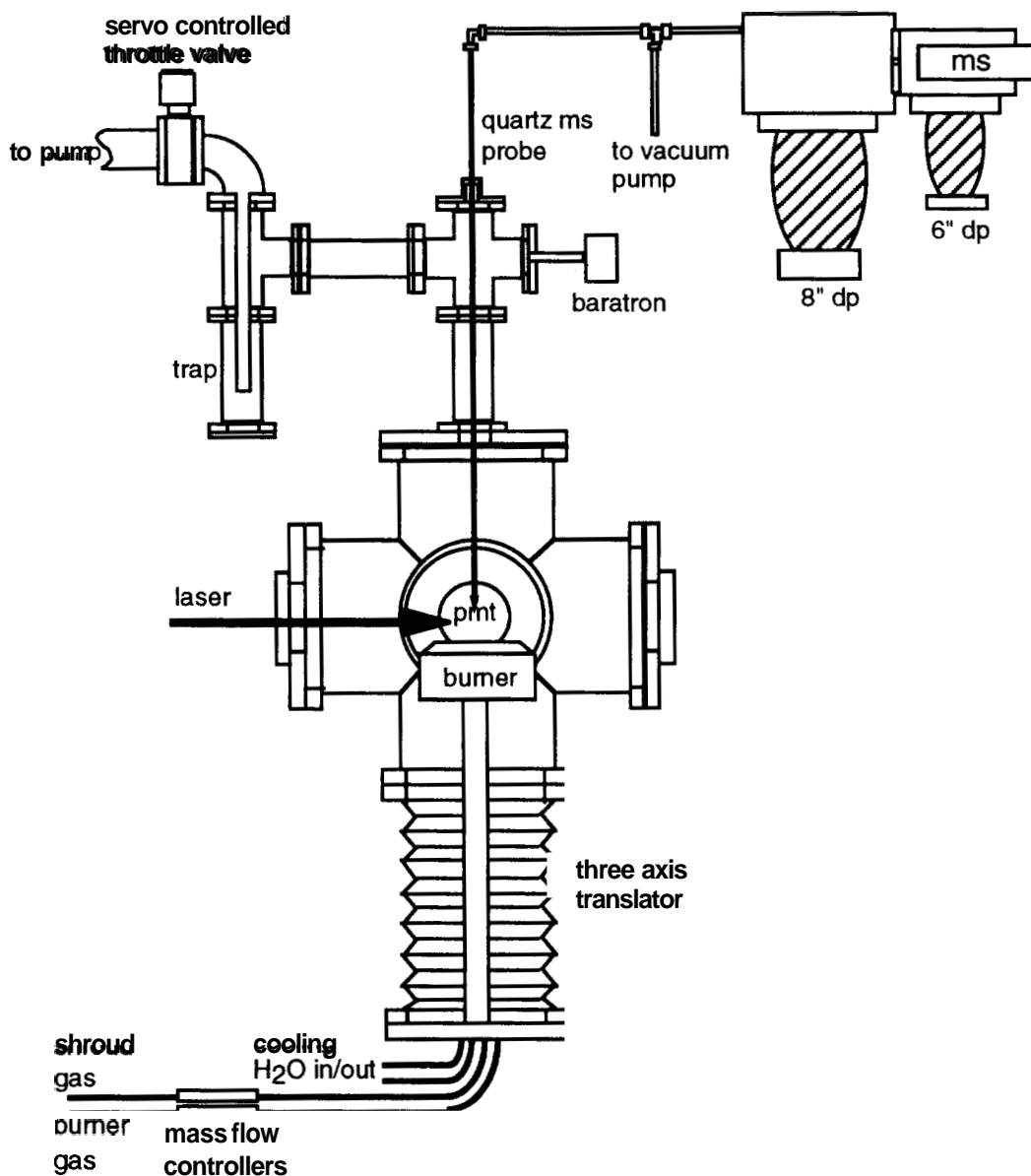
Figure 1: Experimental apparatus.

The four side ports of the flame chamber **are** fitted with 10 cm diameter quartz windows to facilitate spectroscopic investigations. Feedthroughs on these ports also provide access for the igniter and a thermocouple. The igniter is a retractable, resistively heated tungsten element. The thermocouple used to measure flame temperature profiles is a platinum/platinum-rhodium junction home-built from 127 μm diameter wire. To avoid excessive cooling of the flame **gases,** the ceramic insulation ends **4** cm from the thermocouple **tip** leaving only the fine wire to be inserted into the flame. This arrangement minimized flame attachment the thermocouple. However, the unsupported, fine thermocouple wire does droop if left in the flame for extended **periods.**

The gas flows to the burner **are** controlled by **MKS** mass flow controllers calibrated to a standard flowmeter for the gases in use. The gases **are** mixed in a small manifold before entering the

burner. The chamber pressure is servo controlled using a 100 torr capacitance manometer to provide feedback to a throttle valve on the vacuum pump line. Chamber pressure is mainrained to within 0.1 torr.

We currently employ three diagnostics to determine flame temperature and species concentration profiles. Temperatures are determined with the thermocouple described above and by laser-induced fluorescence (LIF). LIF and mass spectrometry are used to determine species concentration profiles.

Our mass spectrometer (ms) system consists of a flame probe and a separate differentially pumped mass spectrometer. The flame probe is a 1 cm diameter quartz tube drawn to a cone at one end. The cone has a 100 μm sampling orifice. The sampling probe walls are ground down at the tip to minimize thermal mass and the resulting flame perturbations. Plastic tubing then connects the sampling probe to the mass spectrometer chamber inlet and a separate mechanical vacuum pump. The mechanical pump acts to maintain a continuous flow through the sampling orifice and holds the mass spectrometer vacuum system inlet pressure at –1 torr. This vacuum system consists of two chambers. The inlet orifice allows gas to expand into the first chamber where the majority is removed by an 8" diffusion pump. An 5 mm orifice connects the first chamber to the second which is pumped by a 6" diffusion pump. The second chamber houses a VG SXP 300 quadrapole mass spectrometer with multi-channel plate detector, unit mass resolution, and a 300 amu range. We use electron impact ionization with an electron energy of 45 V to minimize parent molecule fragmentation.

The mass spectrometer is used in two modes. To collect survey spectra of the major flame components, single scans over the mass range required are digitized with a Lecroy 9314 oscilloscope. For minor species of particular importance to flame suppression such as hydrogen halides, the mass spectrometer is repetitively scanned over a narrow region of a few amu, and the digital oscilloscope is used to increase the signal to noise ratio by signal averaging.

The laser system for LIF consists of a frequency doubled, Nd:YAG pumped dye laser with a bandwidth of approximately 15 GHz. We probe the A(v=1)←X(v=0) band of OH at approximately 285 nm. The laser light enters and exits the chamber through baffles to reduce scattered light. At the fluorescence of OH is detected with a photomultiplier tube (pmt) mounted at 90^0 to the laser axis. A 15 nm bandpass filter centered at 308 nm is located directly in front of the pmt. A series of baffles reduces the field of view of the pmt to the center 1 cm of the burner. The pmt signal is integrated by a gated boxcar integrator and transferred to the computer controlling the laser scan. A second boxcar integrator monitors the laser power detected by a second pmt immediately after the flame chamber.

Results
We have investigated three flames: 1) an undoped, stoichiometric methandair flame, 2) a stoichiometric methandair flamed doped with 0.33% CF_3I and 3) a stoichiometric methandair flame doped with 0.24% C_3F_8. All experiments are conducted at a chamber pressure of 40 torr and a total flow rate through the burner of 4.48 standard liters per minute (slm). Below we present plots of temperature and relative concentration for major species and halogens as a function of burner height. Fig.2 presents a summary of the temperature profile data and includes a comparison to a 0.33% CF_3Br dope methane/air flame.

We note several general features of our results here. First, the position of the flame front appears to shift between the temperature and concentration measurements. We believe this is due to greater flame attachment to the larger ms probe. Visual observations of the flame front are in accord with this trend in the data. Second, relative concentration profiles are produced as follows: For the major species shown in Figs. 3,4,6, survey mass spectra are recorded along with the inlet pressure

to the ms. For the halogen species in Figs. 5,7, the signals are much lower, and we signal average by repetitively scanning over a small mass range. As we move the probe further from the burner surface, we observe a reduction in inlet pressure. We assume this is a measure of the deviation of the flame from one dimensional behavior. If the flame were truly one dimensional, the flux entering the quartz sampling probe would be constant and so would the inlet pressure. If the flame expands radially as well as accelerating the flow velocity along the flame axis, the flow velocity will not increase as much as needed to keep the flux constant, and the flux will decrease with height above the burner. Thus we use the inlet pressure to correct for the expansion of the flame column. This correction makes comparison to one dimensional flame models more accurate. Finally we note that the species profiles presented here represent the result of cooling the flame gas to room temperature and transporting through 10 m of 1.5 cm id tubing. Thus, no radicals can be detected and stable species concentrations must be interpreted as including contributions from radical recombination.
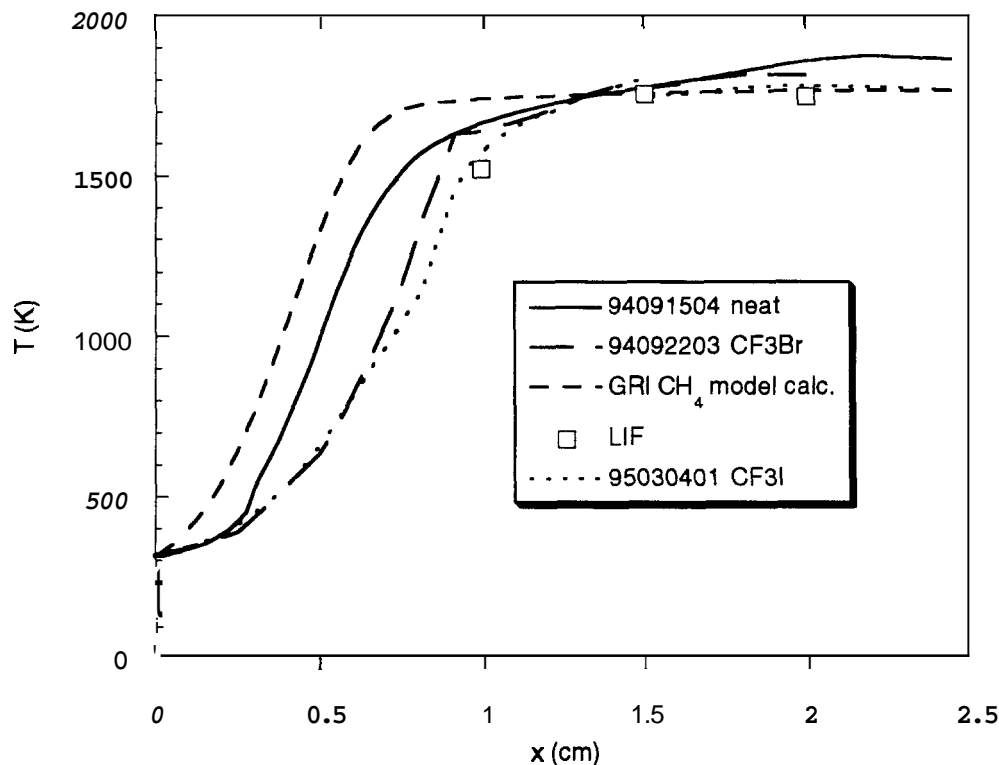

Figure 2: Temperature profiles measured with a $127\mu m$ platinum thermocouple for various flames as a function of height above the burner. Comparison shown with calculated temperature profile using the GRI methane oxidation mechanism[2'] and with OH LIF temperature data.

Stoichiometric CH_4/Air Flame

Fig. 3 displays the relative concentration profiles for oxygen, water, nitrogen, methane and carbon dioxide in a stoichiometric methane air flame at 40.0 torr pressure as measured with our probe sampling mass spectrometer system. The methan air flame is a well known system, and we present these results primarily as a point of comparison for the doped flames presented below. Fig. 3 clearly shows that we have good spatial resolution over the critical flame front region. The essentially flat N_2 profile (displayed as diamonds in Fig. 3) shows that our pressure correction for de-

viations from one dimensional flow is valid. The small bump at the flame front may be due to CH, since we obtain the N, profile from the mass **14** peak. It seems unlikely that methylene reaches our mass spectrometer **as** a radical from the flame front due to our long, high pressure transfer tube. **A** more likely explanation would be that it appears as a fragment ion from a species produced by radical recombination in the probe.
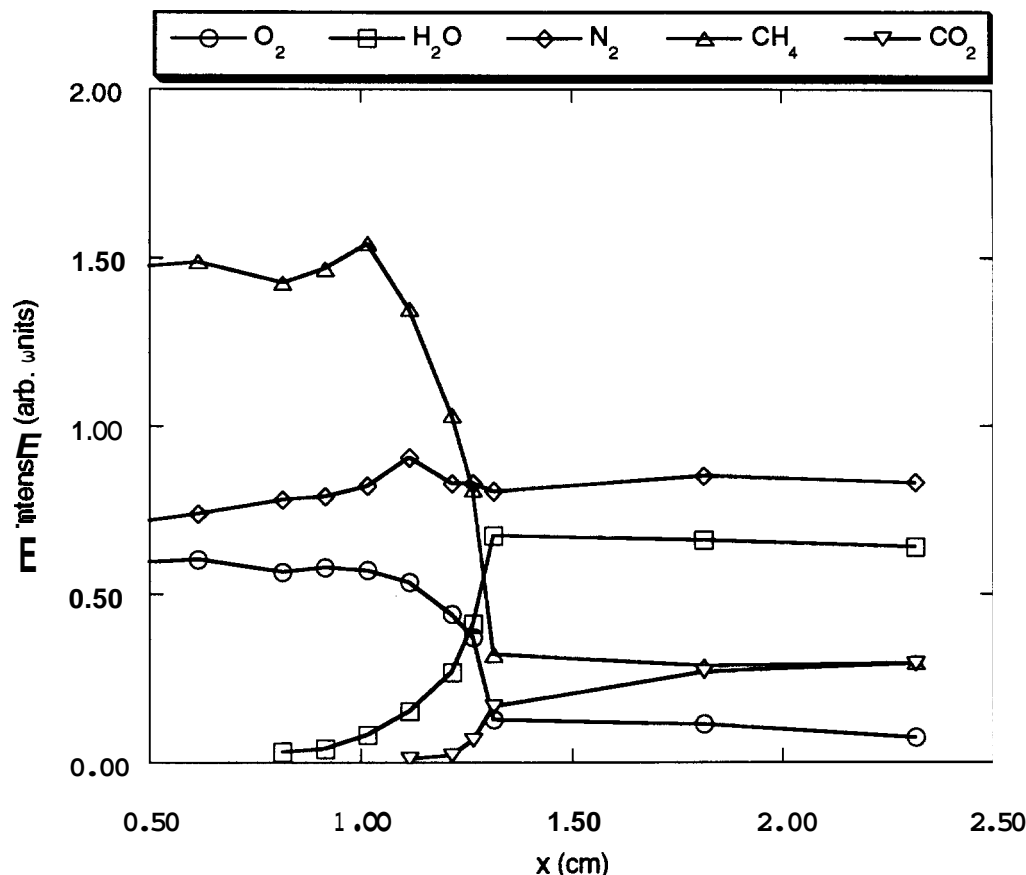

Figure 3: Mass spectral data for the stoichiometric CH_4/air flame at 40.0 torr.

Stoichiometric CH_4/Air Flame Doped With 0.33% CF_3I
We added CF_3I to the stoichiometric methandair flame until the flame became unstable at a pressure of 40 torr and total flow rate of **4.48** slm. We found that 0.33% was the highest fraction of CF_3I with which we could regularly stabilize a flame. Fig. **4** displays the major species for a stoichiometric CH_4/air flame doped with 0.33% CF_3I. Note that the flame front moves further from the burner surface than for the undoped methandair flame (see Fig. 3). This behavior is indicative of flame suppression. Fig. **5** shows the concentration profiles for the F atoms, HF, I atoms and HI. Below the flame zone (x<1.5), the I and F atoms are most likely the result of CF_3I dissociative ionization. The **rise** of I atom intensity at flame zone elevations (1.5<x<2.0) may come from I, fragmentation where I, is the result of I atom recombination in the sampling probe. The I atom signal reaches its peak at x=1.75 cm somewhat ahead of the center of the flame zone at **1.89** cm (as measured from the midway point of the decay of the CH, signal). Note that the F atom signal peaks at approximately the center of the flame zone suggesting that fluorine is liberated from CF_3I more slowly than iodine. This is in good agreement with the relative bond strengths of C-I < C-F. Preliminary model results are in good agreement with these results.
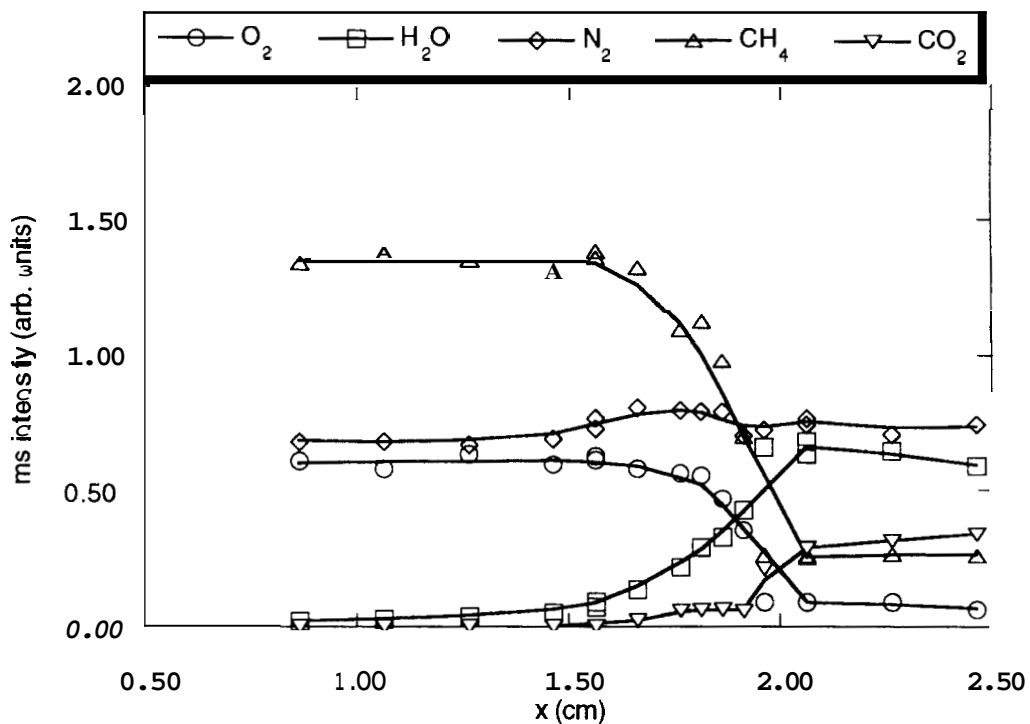
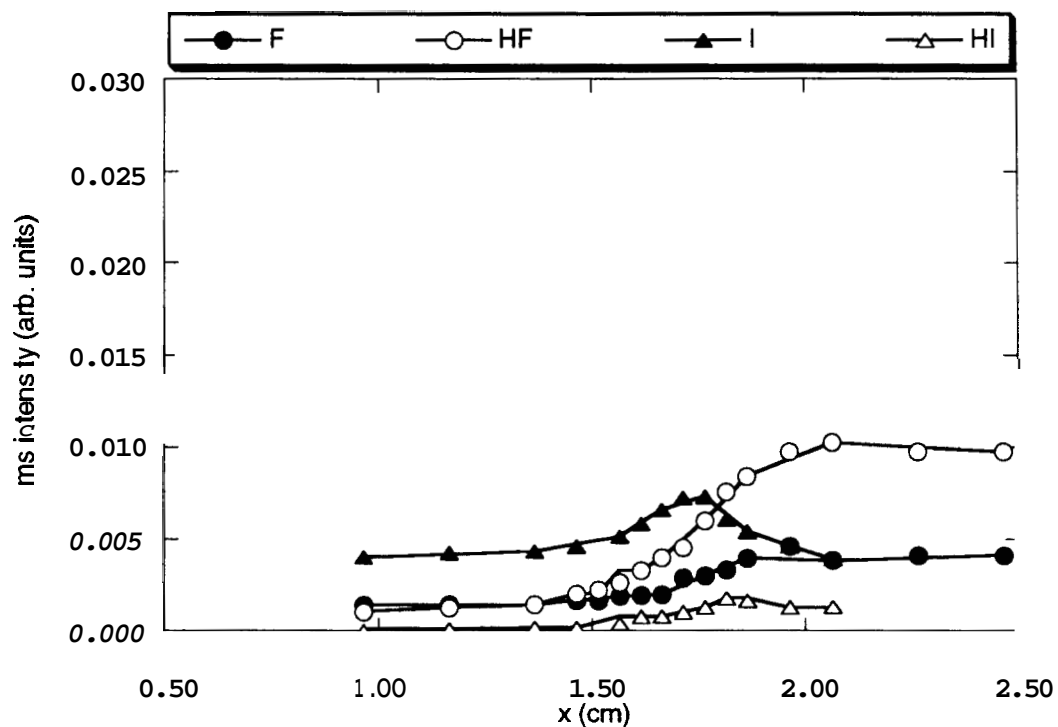Figure **4:** Mass spectral data for the stoichiometric CH_4/air flame at 40.0 torr doped with **0.33%** CF_3I.

Figure 5: Halogen containing species relative concentrations in stoichiometric CF_3I/CH_4/air flame doped with **0.33%** CF_3I.

Stoichiometric CH$_4$/Air Flame Doped With 0.24% C$_3$F$_8$

Our C$_3$F$_8$ studies were somewhat impeded by our flowcontrollers which could not control a steady flow of **0.33%** perfluoropropane as we had hoped. We were instead limited to a maximum flow of 0.24% which we present here. Fig. **6** displays the major species for a stoichiometric CH$_4$/air flame doped with 0.24% C$_3$F$_8$. Fig. 7 shows the concentration profiles for the F atoms and HF plotted on the same relative scale as Fig. 5. Note that the flame front for the C$_3$F$_8$ doped flame further from the burner than for the undoped flame, but closer than for the CF$_3$I doped flame. Although we dope with less C$_3$F$_8$ than CF$_3$I, we show below that this alone does not account for the observed difference. **As** we observed for the CF$_3$I doped flame, we find that the F atom signal again peaks at approximately the center of the flame zone. **As** expected, we find much higher HF concentration in the perfluoropropane post-flame **gases** compared to those of the CF$_3$I doped flame. Normalizing for the different starting concentrations, we find that the ratio of HF produced from flames doped with C$_3$F$_8$ versus CF$_3$I to be 3.2±0.7. Based solely on the per molecule fluorine count, we would expect this ratio to be 8/3=2.7.
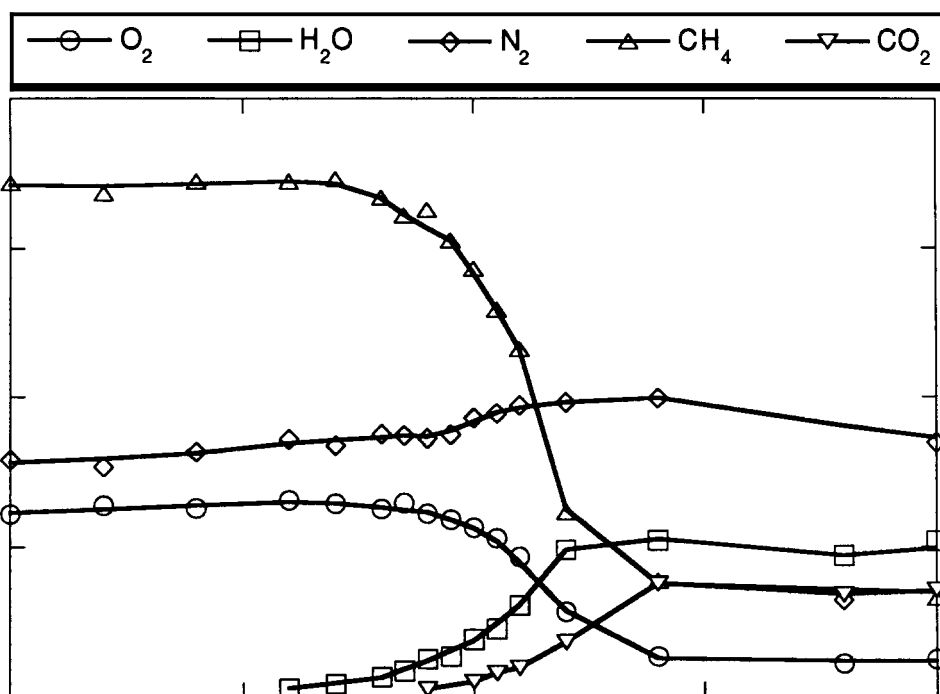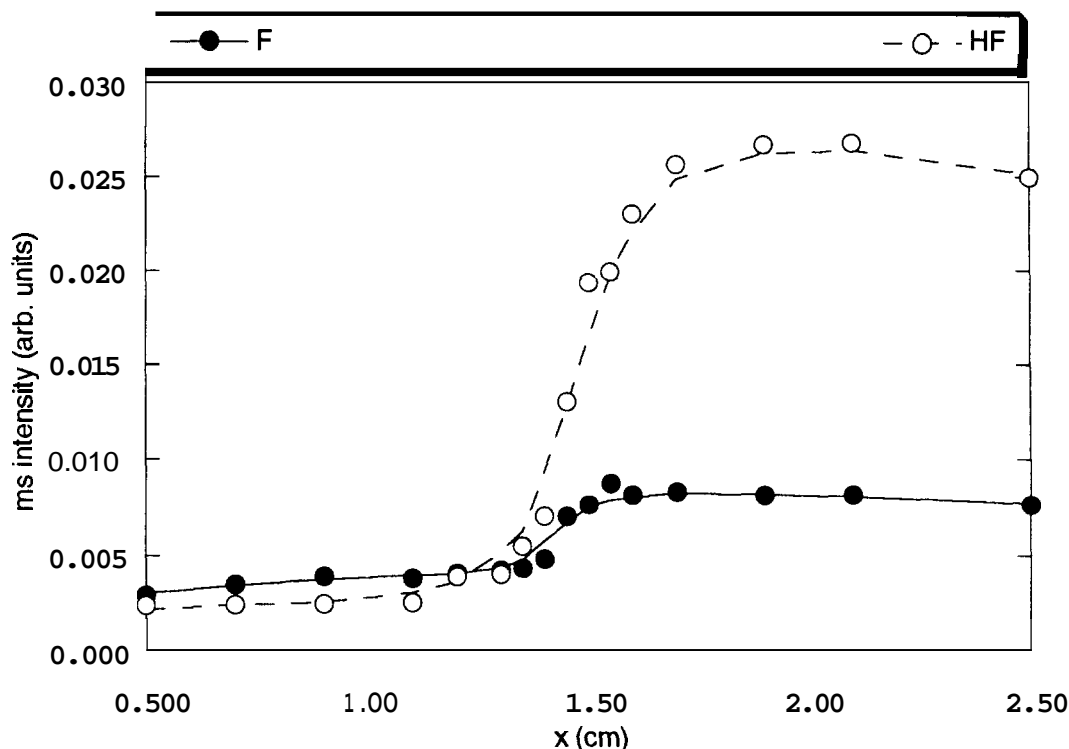
Figure 7: Halogen containing species relative concentrations in a stoichiometric CH_4/air flame doped with 0.24% C_3F_8.

Discussion and Conclusion

We have measured temperature profiles and relative concentration profiles for major species in low pressure flames of CH_4/air, CH_4/air/CF_3I, and CH_4/air/C_3F_8. We find behavior typical of combustion inhibition for flames doped with CF_3I and C_3F_8. The flames are further from the burner and are difficult to stabilize. As the temperature profiles in Fig. 2 show, the rise from the burner is essentially identical for CF_3Br and CF_3I in accord with previous measurements which show similar fire suppression performance.[22] Since different amounts of perfluoropropane and CF_3I are doped in the methandair flames reported here, it is not easy to compare their fire suppression characteristics. If we make a linear extrapolation of the flame front shift from 0.24% to 0.33% perfluoropropane, we find that its the peffluoropropane flame front still appears below the CF_3I flame front indicating poorer fire suppression performance for perfluoropropane. This is again in good agreement with previous results. Table I summarizes these results. As noted above, the HF production from CF_3I and C_3F_8 is approximately proportional to their relative fluorine abundance.

Table I: Flame front positions measured from ms data and predicted.

Flame	Flame Front Position (cm)	Predicted Flame Front (cm)
neat	1.23	
0.24%C_3F_8	1.62	
0.33% C_3F_8		1.77
0.33% CF_3I	1.89	

In Fig. 8, we show the results of preliminary model calculations of major stable species and important halogenated species in the CF_3I doped stoichiometric methandair flame. We use the GRI methane oxidation mechanism[21] coupled with a reduced CF_3X mechanism following Westbrook." We substitute the appropriate iodine reaction rates from the NIST compilations for the bromine rates in Westbrook's work. The Sandia PREMIX flame code[18] is used with our experimentally

determined temperature profile. The model results predict the nearly complete combustion of CF_3I to produce primarily HF and I atoms in the post-flame gases. This is in good agreement with our results. The prediction of residual CF in the flame may be a result of the simplified chemistry used in the model. The post-flame **HI** that we observe in the mass spectrometer is most likely the result of radical reactions in the sampling system. The model also shows the production of **I** atoms early in the flame, 0.25 cm below the peak of water production. We observe the peak in **HI** and I signals in the mass spectrometer 0.20 ± 0.5 *cm* below the water *peak* in good agreement with the calculation.
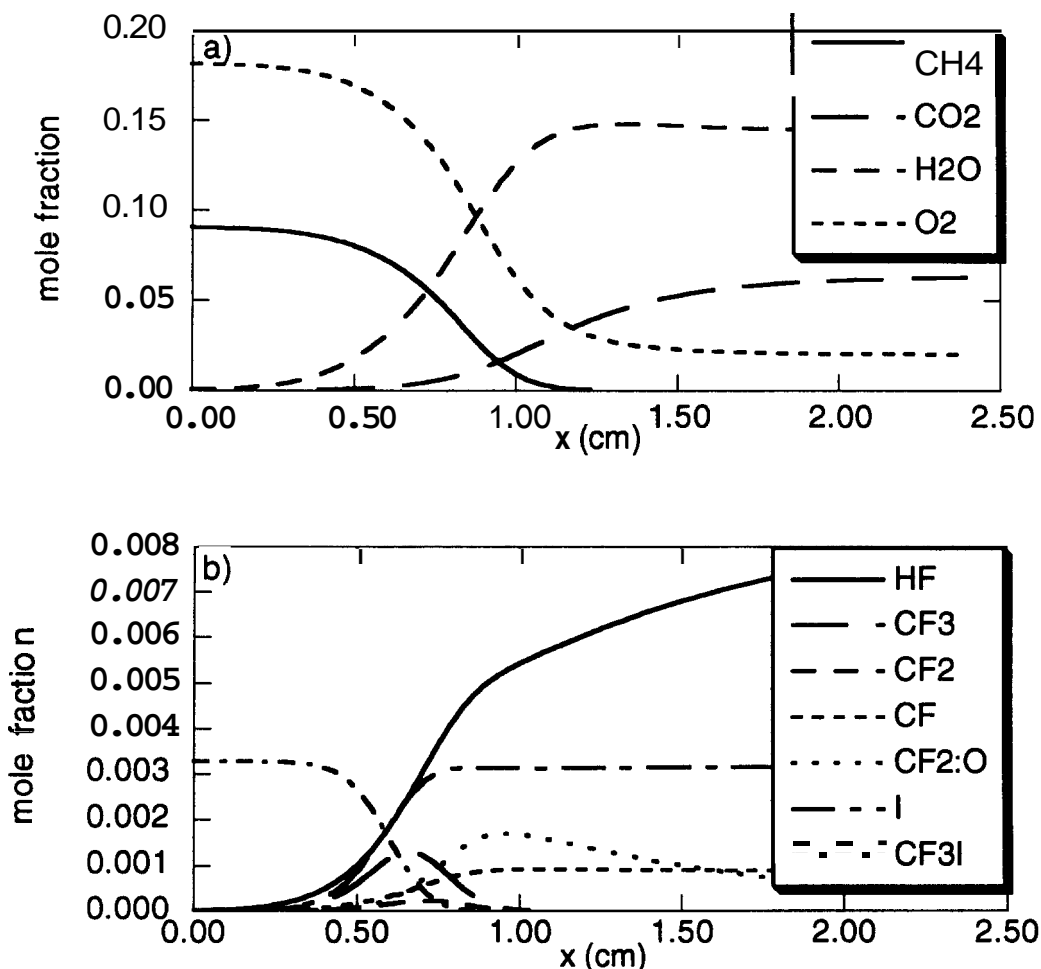

Fig. 8: Results of preliminary one-dimensional, laminar flame model calculations for CF_3I doped methandair flames. a) Shows the predicted concentration profiles for major stable species and b) shows the important halogenated species on an expanded concentration scale. *See* text for details.

The results presented here represent only a preliminary view of the structure of these inhibited flames. Additional work is required to model these results more accurately and to measure the concentration profiles of more species with less perturbation to the flame. One dimensional flame models employing detailed chemical kinetics can be compared to these results to test their validity. Additional **LIF** work needs to be done to measure the **OH** radical concentration profiles as well as other species. We plan to move this experiment to more spacious quarters in the near future which will enable us to locate the mass spectrometer much closer to the flame chamber. We are also designing an improved sampler for the mass spectrometer with lower mass and greater conductance.

Acknowledgments

References

[1] J. C. Biordi, C. P. Lazzara and J. F. Papp, U. S. Bur. Mines Rept. of Investigations RI8029 (1975).

[2] J. C. Biordi, C. P. Lazzara and J. F. Papp, *Fifteenth Symposium (International)on Combustion,* The Combustion Institute, Pittsburgh, PA, 1975, 917.

[3] J. C. Biordi, C. P. Lazzara and J. F. Papp, *J. Phys. Chem.* **81,** 1139 (1977).

[4] J. C. Biordi, C. P. Lazzara and J. F. Papp, *J. Phys. Chem.* **82,** 125 (1978).

[5] M. J. Day, D. V. Stamp, K. Thompson, and G. Dixon Lewis, *Thirteenth Symposium (International)on Combustion,* The Combustion Institute, Pittsburgh, PA, 1971, 705.

[6] G. Dixon Lewis and R. J. Simpson, *Sixteenth Symposium (International)on Combustion,* The Combustion Institute, Pittsburgh, PA, 1977, 1111.

[7] G. Dixon Lewis, *Combustion and Flame* **36,** 1979, 1.

[8] C. K. Westbrook, *Nineteenth Symposium (International) on Combustion,* The Combustion Institute, Pittsburgh, PA. 1982, 127.

[9] C. K. Westbrook, *Combustion Science and Technology* **23,** 191 (1980).

[10] C. K. Westbrook. *Combustion Science and Technology* **34,** 201 (1983).

[11] R. S. Sheinson, J. E. Penner-Hahn. and D. Indritz, *Fire Safety Journal* **15,** 437 (1989).

[12] F. Battin-Leclerc, G. M. Come, and F. Baronnet, *Combustion and Flame* **99,** 644 (1994).

[13] V. 1. Babushok, D. R. F. Burgess, Jr., and W. Tsang, *Halon Options Technical Working Conference Proceedings,* Albuquerque, NM, 1994,205.

[14] R. G. Daniel, K. L. McNesby, A. W. Miziolek, D. R. F. Burgess, Jr., P. R. Westmoreland, W. Tsang, and M. R. Zachariah. *Halon Options Technical Working Conference Proceedings, Albuquerque, NM,* 1994, 229.

[15] G. T. Linteris, M. D. King, A. Liu, C. Womeldorf, and Y. E. Hsin, Halon Options Technical Working Conference Proceedings, Albuquerque, NM, 1994, 177.

[16] G. T. Linteris, and L. Truett, *Halon Options Technical Working Conference Proceedings,* Albuquerque, NM, 1994, 217.

[17] R. J. Kee, J. F. Grcar, M. D. Smooke, and J. A. Miller, SAND85-8240.UC-4 Sandia National Laboratory, Albuquerque, NM 1987.

[18] R. J. Kee, G. Dixon-Lewis, J. Warnatz, M. E. Coltrin, and J. A. Miller, SAND86-8246.UC-32 Sandia National Laboratory, Albuquerque, NM 1986.

[19] R. J. Kee, F. M. Rupley and J. A. Miller, SAND89-8009.UC-401 Sandia National Laboratory, Albuquerque, NM 1991.

[20] R. J. Kee, F. M. Rupley and J. A. Miller, SAND87-8251B.UC-4 Sandia National Laboratory, Albuquerque, NM 1991.

[21] G. P. Smith, M. Frenklach, H. Wang, T. Bowman, D. Golden, W. Gardiner, V. Lissianski, and R. Serauskas, Methane Combustion Kinetics Mechanism Version 1.1, sponsored by the Gas Research Institute, available via anonymous ftp from CRVAX.SFU.COM.

[22] C. J. Kibert, *Halon Opnons Technical Working Conference Proceedings,* Albuquerque, NM, 1994. 261.